

## Wetting in Hydrophobic Nanochannels: A Challenge of Classical Capillarity

Roy Helmy, Yuri Kazakevich, Chaoying Ni,<sup>†</sup> and Alexander Y. Fadeev\**Department of Chemistry and Biochemistry, Seton Hall University, South Orange, New Jersey 07079, and  
Department of Materials Science and Engineering, University of Delaware, Newark, Delaware 19716*

Received May 18, 2005; E-mail: fadeeval@shu.edu

The structure of the water–hydrophobic interface is of fundamental interest for the understanding of biological and colloidal systems. Due to the perturbation of the hydrogen bonding, the structure of water near a hydrophobic surface is quite different from the bulk; in particular, the presence of a density depletion layer at the interface has been suggested.<sup>1–3</sup> Direct experimental characterization of this interface, however, is difficult, and the few reported results are varied.<sup>4–7</sup>

Here, we report investigation of a water–hydrophobic interface in nanochannels. Due to a large interface ( $\sim 10^2$ – $10^3$  m<sup>2</sup>/g), a substantial amount of excess interfacial energy can be accumulated in such systems,<sup>8</sup> leading to interesting applications for storage and dumping of mechanical energy.<sup>9</sup> We studied the intrusion of water in hydrophobic nanochannels (Figure 1), using the water porosimetry technique described in previous work.<sup>10</sup> A series of ordered mesoporous silicas (SBA type,  $R_{\text{pore}} \approx 2$ – $4$  nm) was prepared and hydrophobized with the monolayers of trimethylsilyl groups (TMS). Using these well-defined porous solids as models, we demonstrated that classical (macroscopic) theory fails to describe wetting at nanoscale. The results suggested the presence of a thin vapor (low-density) layer separating water and the hydrophobic surface.

A typical water intrusion ( $P$ – $V$ ) diagram (Figure 2) of the TMS-silicas showed two steps: (i) filling of the interparticle voids ( $< 3$  MPa) and (ii) the pore filling with water ( $\sim 20$ – $40$  MPa). The values of  $P_{\text{INTR}}$  and  $V_{\text{H}_2\text{O}}$  showed virtually no dependence on the rate of compression ( $\sim 4$ – $27$  MPa/min) or contact time ( $1$ – $24$  h), suggesting that the process was close to the equilibrium.<sup>11</sup> The values of  $P_{\text{INTR}}$  and  $V_{\text{H}_2\text{O}}$  are provided in the Supporting Information.

In classical theory of capillarity, the pressure required to push a nonwetting liquid into a cylindrical pore with radius  $R$  is determined by the Laplace equation:

$$P_{\text{INTR}} = P_l - P_v = -\left(\frac{2\gamma}{R}\right) \cos \theta \quad (1)$$

where  $\gamma$  is surface tension,  $P_l$  and  $P_v$  are pressures in the liquid and vapor phases, respectively. Using eq 1, one assumes that, inside the pores, the liquid meets the solid at the angle  $\theta$ , which is equal to the macroscopic (Young's) contact angle for the liquid on a flat surface with composition similar to that inside the pores. This assumption, although commonly made, is hardly valid, however, as the profile of the liquid near the solid surface ( $\sim$ nm range) is complex and cannot be described by a single contact angle. We found that eq 1 (using the advancing water contact angle of  $106^\circ$ , a well-established value for the TMS monolayers<sup>12</sup>) gave intrusion pressures  $\sim 1.5$ – $2$  times smaller than in the experiment (Figure 3). The data would fit eq 1, once the "apparent water contact angle" of  $\sim 120^\circ$  was assumed.<sup>13</sup> We note, however, that the contact angle  $\sim 120^\circ$  is unreasonably high for the TMS surface and is rather

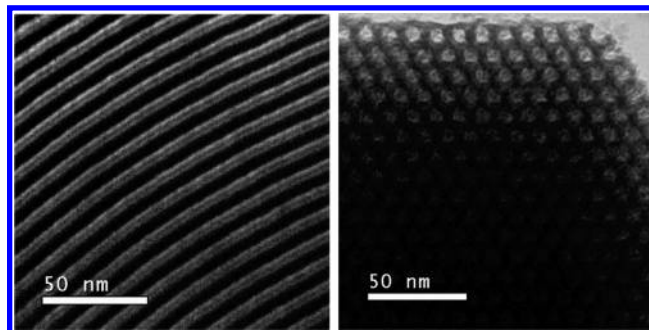


Figure 1. TEM micrographs of porous silica.

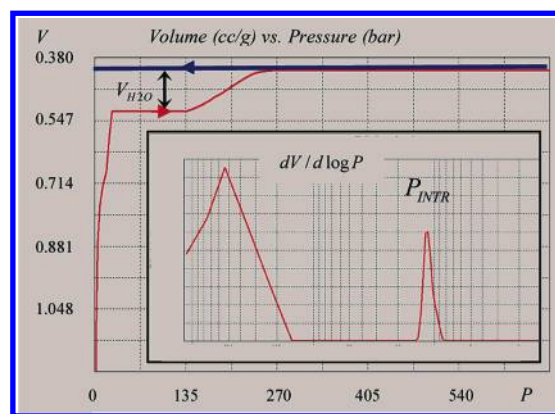


Figure 2. Water intrusion ( $P$ – $V$ ) diagram for the TMS-silica. Differential plot  $dV/(d \log P)$  (inset) shows peaks  $\sim 27$  bar (interparticle voids) and  $\sim 200$  bar (pore filling).

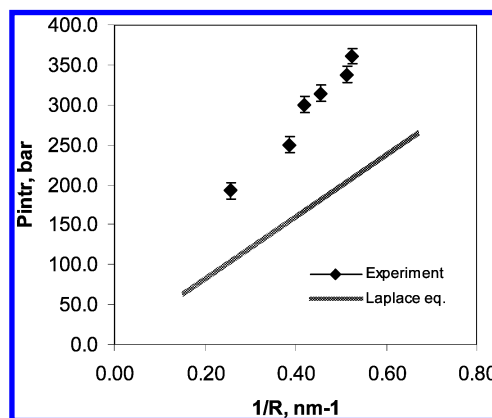
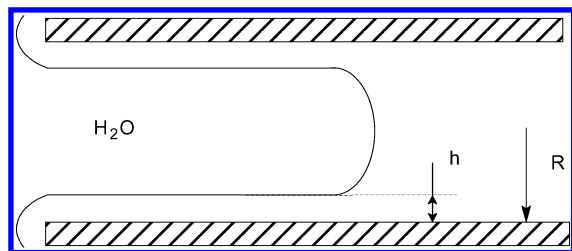


Figure 3. Water intrusion pressure plotted vs  $1/R$  of a hydrophobic pore, characteristic for surfaces of fluorinated alkyls.<sup>15</sup> One may argue that the contact angles in pores are increased due to the effects of surface roughness. The surfaces prepared in this work are quite smooth (Figure 1), and only subnanometer roughness can be present inside the pores, which is too small to cause significant change in the contact angles.

<sup>†</sup> University of Delaware.



**Figure 4.** Water (nonwetting fluid) in a hydrophobic pore is separated from the walls by a thin layer of vapor/low-density film (wetting fluid).

Our second observation that could not be explained from the standpoint of classical capillarity was related to the pore volume. The pore volumes of the TMS-silicas available to water ( $V_{\text{H}_2\text{O}}$ ) were notably smaller (on average  $\sim 60\%$ ) than the pore volumes measured by nitrogen adsorption ( $V_{\text{N}_2}$ ). Such a reduction in pore volume could not be explained by the elastic deformations of silicas under pressure. We determined the compressibility of the TMS-silicas to be  $\sim 10^{-4} \text{ MPa}^{-1}$ ; thus, in the pressure range  $\sim 20\text{--}40 \text{ MPa}$ , the elastic deformation of the matrix is only  $\sim 2\text{--}4\%$  (by volume). Given the simple pore geometry, the observed difference in the pore volumes suggests the presence of a layer of low-density fluid separating the water from the pore walls (Figure 4). The thickness of this layer can be determined as follows:

$$h = R_{\text{TMS}} \left( 1 - \sqrt{\frac{V_{\text{H}_2\text{O}}}{V_{\text{N}_2}}} \right) \quad (2)$$

The values of thickness ranged from 0.42 to 0.64 nm with the average value of  $0.56 \pm 0.09 \text{ nm}$ .

The presence of a vapor (low-density) film separating water from the hydrophobic walls can be rationalized in terms of Derjaguin's surface thermodynamics and disjoining pressure.<sup>16,17</sup> In a hydrophobic pore, the vapor phase is the wetting fluid, which, at the equilibrium, forms wetting film with thickness  $h$  (Figure 4).<sup>18</sup> For water in a cylindrical hydrophobic pore, the pressure equilibrium is determined by the balance of capillary pressure and disjoining pressure ( $\Pi(h)$ ) in the wetting film:

$$P_{\text{INTR}} = P_1 - P_v = \frac{\gamma}{R - h} + \Pi(h) \quad (3)$$

Treating the vapor film as a van der Waals fluid, the equation for the disjoining pressure  $\Pi(h) = A/(6\pi \cdot h^3)$  can be used:

$$P_{\text{INTR}} = P_1 - P_v = \frac{\gamma}{R - h} + \frac{A}{6\pi \cdot h^3} \quad (4)$$

where  $A$  is the Hamaker constant. Using the values of the film thickness  $h$  obtained from the pore volume data (eq 2), the best fit of the intrusion pressures gives  $\sim 7.5 \pm 1.8 \times 10^{-20} \text{ J}$  for the Hamaker constant. This value is in a reasonable agreement with the values expected for the hydrophobic solid interacting with water across the vapor gap.<sup>19</sup>

In summary, the classical (macroscopic) theory of capillarity (Laplace) fails to accurately describe the water–hydrophobic interface in nanopores. The results suggest the presence of  $\sim 0.6 \text{ nm}$  low-density fluid (vapor film) separating water from the hydrophobic solid. The presence of this layer is rationalized in terms of Derjaguin's surface thermodynamics and disjoining pressure.

**Acknowledgment.** We acknowledge support from the NSF (CMS-0304098). Dr. Konstantin Kornev (TRI/Princeton) is acknowledged for valuable comments. Ms. Megan Kouba (Seton Hall) is acknowledged for the synthesis of silicas.

**Supporting Information Available:** Experimental details on synthesis and characterization of TMS-silicas ( $\text{N}_2$  adsorption, TEM, and water intrusion). This material is available free of charge via the Internet at <http://pubs.acs.org>.

## References

- (1) Stillinger, F. H. *J. Solution Chem.* **1973**, *2*, 141.
- (2) Ruckenstein, E.; Churaev, N. V. *J. Colloid Interface Sci.* **1991**, *147*, 535.
- (3) Lum, K.; Chandler, D.; Weeks, J. D. *J. Phys. Chem. B* **1999**, *103*, 4570.
- (4) Jensen, T. R.; Jensen, M. O.; Reitzel, N.; Balashev, K.; Peters, G. H.; Kjaer, K.; Bjørnholm, T. *Phys. Rev. Lett.* **2003**, *90*, 086101.
- (5) Schwendel, D.; Hayashi, T.; Dahint, R.; Pertsin, A.; Grunze, M.; Steitz, R.; Schreiber, F. *Langmuir* **2003**, *19*, 2284.
- (6) Steitz, R.; Gutberlet, T.; Hauss, T.; Klösgen, B.; Krastev, R.; Schemmel, S.; Simonsen, A. C.; Findenegg, G. H. *Langmuir* **2003**, *19*, 2409.
- (7) Sur, U. K.; Lakshminarayanan, V. *J. Electroanal. Chem.* **2004**, *565*, 343.
- (8) Bogomolov, V. N. *Phys. Rev. B* **1995**, *51*, 17040.
- (9) Eroshenko, V. A.; Regis, R. C.; Soulard, M.; Patarin, J. *J. Am. Chem. Soc.* **2001**, *123*, 8129.
- (10) Fadeev, A. Y.; Eroshenko, V. A. *J. Colloid Interface Sci.* **1997**, *187*, 275.
- (11) It is noted that significant hysteresis was present in the system: when the pressure was dropped back to atmospheric, water did not come out of the pores. This water was loosely bound with the surface, and it could be easily removed by heating ( $\sim 50^\circ \text{C}$ ) or by evacuation. We also note that the retention of water in pores was not due to changes of the porous structure or the surface chemistry (hydrolysis). Once water was removed from the pores, the shape of the intrusion programs, including intrusion pressure and intrusion volume, were reproduced in the consecutive intrusion experiments. Nitrogen adsorption isotherms of the samples before and after water intrusion were practically unchanged, indicating that the porous structure was not affected by the intrusion. At this point we offer no explanation of the hysteresis in these systems, and we continue research to address this question.
- (12) Fadeev, A. Y.; McCarthy, T. J. *Langmuir* **1999**, *15*, 3759.
- (13) Contact angles of  $\sim 120\text{--}140^\circ$  were determined (from eq 1) for the intrusion of water in silica gels hydrophobized with alkylsilanes ( $\text{C}_1$  to  $\text{C}_{16}$ )<sup>10</sup> and for  $\text{C}_8\text{-MCM41}$  silicas.<sup>14</sup> These values of contact angles are too high for the monolayers of alkyldimethylsilanes (realistic values<sup>12</sup>  $\sim 100\text{--}106^\circ/90\text{--}98^\circ$ , advancing/receding).
- (14) Lefevre, B.; Saugey, A.; Barat, J. L.; Bocquet, L.; Charlaix, E.; Gobin, P. F.; Vigier, G. *J. Chem. Phys.* **2004**, *120*, 4927.
- (15) Zisman, W. A. *Advances in Chemistry Series 43*; American Chemical Society, 1964; p 1.
- (16) Derjaguin, B. V.; Churaev, N. V.; Muller, V. M. *Surface Forces*. Consultant Bureau, NY-London, 1987.
- (17) Churaev, N. V. *Adv. Colloid Interface Sci.* **2003**, *103*, 197.
- (18) The presence of the low-density fluid is not unique to water and hydrophobic surfaces; in fact, it is expected for all lyophobic solid–liquid interfaces. To support this statement, a gap  $\sim 0.1\text{--}0.2 \text{ nm}$  separating solid and nonwetting liquid was reported for the intrusion of liquid metals and melts (Hg, Bi, Pb, Cd, In, Ga) in porous zeolites.<sup>8</sup>
- (19) The Hamaker constant for the hydrophobic solid interacting with water across the vapor gap was estimated from combining rule:  $A_{132} = (\sqrt{A_{11}} - \sqrt{A_{33}})(\sqrt{A_{22}} - \sqrt{A_{33}}) \approx 5.1 \times 10^{-20} \text{ J}$  using the following values of Hamaker constants ( $10^{-20} \text{ J}$ ): 7.1 (hydrocarbon, media 1), 3.7 (water, media 2), and 0 (vapor, media 3). Israelashvili, J. *Intermolecular and Surface Forces*, 2nd ed.; Academic Press, 1992.

JA053267C